

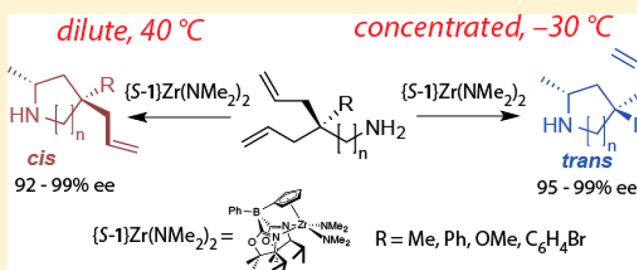
# Zirconium-Catalyzed Desymmetrization of Aminodialkenes and Aminodialkynes through Enantioselective Hydroamination

Kuntal Manna,<sup>†</sup> Naresh Eedugurala, and Aaron D. Sadow\*

U.S. Department of Energy Ames Laboratory and Department of Chemistry, Iowa State University, 1605 Gilman Hall, Ames, Iowa 50011, United States

**S** Supporting Information

**ABSTRACT:** The catalytic addition of alkenes and amines (hydroamination) typically provides  $\alpha$ - or  $\beta$ -amino stereocenters directly through C–N or C–H bond formation. Alternatively, desymmetrization reactions of symmetrical aminodialkenes or aminodialkynes provide access to stereogenic centers with the position controlled by the substrate's structure. In the present study of an enantioselective zirconium-catalyzed hydroamination, stereocenters resulting from C–N bond formation and desymmetrization of a prochiral quaternary center are independently controlled by the catalyst and reaction conditions. Using a single catalyst, the method provides selective access to either diastereomer of optically enriched five-, six-, and seven-membered cyclic amines from aminodialkenes and enantioselective synthesis of five-, six-, and seven-membered cyclic imines from aminodialkynes. Experiments on hydroamination of aminodialkenes testing the effects of the catalyst:substrate ratio, the absolute concentration of the catalyst, and the absolute initial concentration of the primary amine substrate show that the latter parameter strongly influences the stereoselectivity of the desymmetrization process, whereas the absolute configuration of the  $\alpha$ -amino stereocenter generated by C–N bond formation is not affected by these parameters. Interestingly, isotopic substitution ( $\text{H}_2\text{NR}$  vs  $\text{D}_2\text{NR}$ ) of the substrate enhances the stereoselectivity of the enantioselective and diastereoselective processes in aminodialkene cyclization and the peripheral stereocenter in aminodialkyne desymmetrization/cyclization.



## INTRODUCTION

Carbon–nitrogen bond-forming reactions involving the addition of amines and unsaturated hydrocarbons, known as hydroamination, are developing into useful and complementary synthetic alternatives to important reductive amination and cross-coupling methods.<sup>1–4</sup> Stereoselective addition of an NH functionality to an olefin typically provides chiral amines with  $\alpha$ - and/or  $\beta$ -amino stereogenic centers resulting from corresponding C–N and/or C–H bond formation, and the locations of these stereocenters inherently limit the structural features of products available with catalytic hydroamination methods. Additional stereocenters are typically installed through prior or subsequent steps, often resulting in significant synthetic complexity and inefficiencies. Thus, the synthetic utility of stereoselective hydroamination could be further improved by single-step assembly of multiple stereocenters and control over distant stereocenters in the amine products.

One approach to address this problem involves tandem C–N/C–C or C–N/C–N bond formations.<sup>2,5,6</sup> In these transformations, the configuration of the first stereocenter typically governs the selectivity of subsequent C–N or C–C bond forming steps. Alternatively, kinetic resolutions of chiral aminoalkenes provide dialkylpyrrolidines; however, intramolecular resolutions are limited by an accurately timed reaction quench and a maximum possible 50% yield.<sup>7</sup> Alternatively,

multicatalyst sequences involving alkyne hydroamination followed by asymmetric hydrogenation provided a route to optically active morpholine derivatives.<sup>8</sup> In this approach, the hydroamination event dictates the location of the stereocenter, even though the stereocenter's configuration is established in a subsequent step.

Alternatively, desymmetrization is an interesting and effective approach for introducing structural and stereochemical complexity because it readily provides quaternary stereogenic carbon centers.<sup>9,10</sup> This idea is highlighted by examples in ring-closing metathesis of trienes,<sup>11</sup> esterification of symmetric diols,<sup>12</sup> conjugate addition,<sup>13,14</sup> Ullmann coupling,<sup>15</sup> Suzuki coupling,<sup>16</sup> allylic substitution,<sup>17</sup> silylation of diols,<sup>18</sup> and oxidation.<sup>19</sup> Notably, C–C or C–N bonds are not formed or broken at the stereogenic center obtained through desymmetrization.

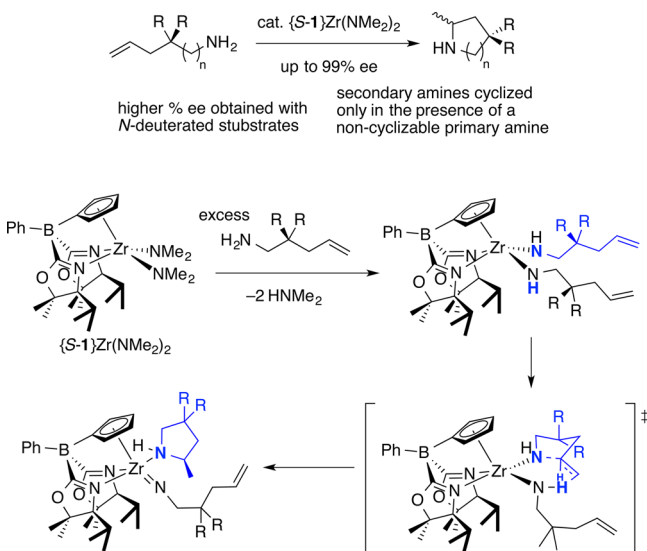
An interesting approach, then, for the synthesis of optically active amines involves enantioselective desymmetrization of dialkenes and dialkynes via hydroamination. This approach has barely been explored. Typically, enantioselective hydroamination reactions of dialkenes occur with poor diastereoselectivity,<sup>7,20–24</sup> and diastereoselective catalysts have not yet been

Received: November 2, 2014

Published: January 2, 2015

modified into effective optically active analogues.<sup>25–27</sup> Notably, a gold(I)-catalyzed desymmetrization of dialkynyl tosylamides provides optically active 2-methylenepyrrolidines in a promising method.<sup>28</sup> In addition, an achiral Ag(I) complex catalyzes the desymmetrization of aminodiyne to racemic 1-pyrrolidines in route to  $\pm$  Monomorine I.<sup>29</sup> That is, the combination of highly enantioselective and diastereoselective hydroamination has not previously been realized in a desymmetrization reaction.

Our previously reported oxazolonylborate zirconium catalyst  $\{\text{PhB}(\text{Ox}^{4S-i\text{PrMe}_2})_2\text{C}_5\text{H}_4\}\text{Zr}(\text{NMe}_2)_2$  ( $\{S-1\}\text{Zr}(\text{NMe}_2)_2$ ) gives high enantioselectivity in hydroamination of aminoalkenes (Figure 1), and this high enantioselectivity is maintained in the



**Figure 1.** Cyclization of aminoalkenes, the conversion of the zirconium precatalyst  $\{S-1\}\text{Zr}(\text{NMe}_2)_2$  to the active species for hydroamination/cyclization of aminoalkenes, and the elementary step proposed for C–N bond formation.

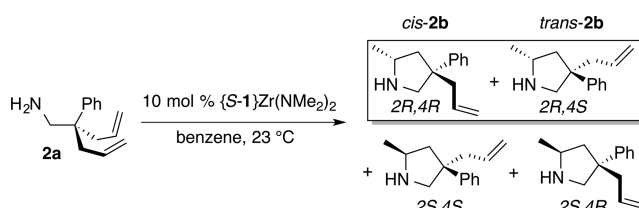
cyclization of nonconjugated aminodialkenes that tended to give poor diastereoselectivity.<sup>20</sup> In previous studies of this zirconium catalyst, we have established the experimental parameters that affect the enantioselectivity of the hydroamination/cyclization reactions. Namely, N-deuterated amine substrates are cyclized with higher enantioselectivity than per-proteo analogues, the concentration of the reaction mixture does not significantly affect the enantioselectivity, and the products' % ee is highest up to  $\sim 80\%$  conversion. In addition, 2 equiv of primary amine are required in the active catalytic site for cyclization to occur, and neither  $\{S-1\}\text{ZrCl}(\text{NMe}_2)$  nor the mono-oxazoline-based compound  $\{\text{Ph}_2\text{B}(\text{Ox}^{4S-i\text{PrMe}_2})\text{C}_5\text{H}_4\}\text{Zr}(\text{NMe}_2)_2$  are viable precatalysts under the conditions that were tested. On the basis of these data and extensive kinetic studies, we previously postulated a pathway for cyclization involving the bis(primary amido)-zirconium species transferring a proton concurrently with N–C bond formation, as shown in Figure 1.

Here we report strategies to control the configuration of the stereocenter formed by desymmetrization of aminodialkenes and aminodialkynes. Significantly, these reactions provide control over quaternary stereogenic centers that are remote from the new C–N bonds. Moreover, the high enantioselectivity associated with this zirconium catalyst is maintained in the desymmetrization reactions, allowing efficient formation of

multiple stereogenic centers in a single catalytic step. Notably, the configurations of these stereocenters are independently controlled by catalyst (for N–H addition) and reaction conditions (desymmetrization). Studies of the effects of isotopic substitution and kinetic measurements provide support for a proposed catalytic pathway.

## RESULTS AND DISCUSSION

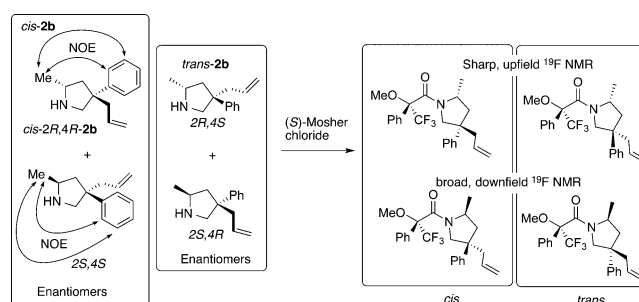
The cyclization of several prochiral diallyl amines ( $\text{H}_2\text{NCH}_2\text{CR}(\text{CH}_2\text{CH}=\text{CH}_2)_2$ ; R = Ph (**2a**), Me (**3a**),  $\text{C}_6\text{H}_4\text{Br}$  (**4a**)) into 4-allyl-2-methylpyrrolidines is catalyzed by bis(dimethylamido) zirconium(IV) coordinated by cyclopentadienyl-bis(oxazolonyl)borate ligands (Figure 2).<sup>20</sup> The pyrroli-



**Figure 2.** Catalytic desymmetrization of an aminodialkene with  $\{S-1\}\text{Zr}(\text{NMe}_2)_2$ . The isomers in the box are the two favored enantiomers.

dine products are formed as a mixture of two diastereomers containing stereocenters at the C2 position resulting from C–N bond formation and at the C4 position generated by desymmetrization of the prochiral tetrahedral center. Four isomers are possible in total as enantiomeric pairs of two diastereomers. For example with R = Ph, the diastereomeric ratio (d.r.) is 3.3:1 as determined by integration of the 2-Me signals in  $^1\text{H}$  NMR spectrum of the crude reaction product. That d.r. is obtained using 10 mol %  $\{S-1\}\text{Zr}(\text{NMe}_2)_2$  (6.5 mM) as the catalyst at room temperature. As reported previously, the % ee of both the major and minor diastereomers is high (96% and 95%), and the 2R configuration is favored in both diastereomers as a result of catalyst-controlled enantioselective C–N bond formation.

The major diastereomer is assigned as *cis* based on NOE correlations between the 2-methyl signal at 1.00 ppm and 4-phenyl *ortho* and *meta* resonances at 7.27 and 6.69 ppm (Figure 3). Reaction of the pyrrolidine **2b** mixture (of enantiomeric



**Figure 3.**  $^1\text{H}$  NOE correlations in *cis*-4-allyl-2-methyl-4-phenylpyrrolidine and  $^{19}\text{F}$  NMR signals of Mosher amide products used to assign C2 and C4 stereochemistry. Ratios of *cis* and *trans* diastereomers for the pyrrolidine were determined by  $^1\text{H}$  NMR spectroscopy, and relative signal intensity of  $^{19}\text{F}$  NMR signals of Mosher amide derivatives of racemic and optically enriched samples were used to assign stereochemistry for each enantiomer.

pairs of two diastereomers) with optically pure Mosher chloride ( $S$ -Ph(OMe)(CF<sub>3</sub>)CCOCl) gives four diastereomeric Mosher amides.

A racemic reaction mixture is obtained from cyclization of **2a** ([**2a**] = 95.8 mM) using the achiral precatalyst {PhB(Ox<sup>Me</sup>)<sub>2</sub>C<sub>5</sub>H<sub>4</sub>}Zr(NMe<sub>2</sub>)<sub>2</sub>. The racemic products from that reaction are obtained as a 3.5:1 mixture of diastereomers.

In this mixture, the enantiomeric pairs are readily assigned in the <sup>19</sup>F NMR spectrum of their Mosher amide derivatives because their resonances necessarily integrate 1:1. The two higher integrating resonances in the <sup>19</sup>F NMR spectrum of the Mosher amides are derived from the *RR* and *SS* enantiomers of the *cis* diastereomeric pair (i.e., *2R,4R,R*<sup>Mosher</sup> and *2S,4S,R*<sup>Mosher</sup>). The minor *trans* diastereomeric pair of enantiomers (*RS/SR*) from the racemic reaction mixture gives the second set of two equal-intensity <sup>19</sup>F NMR resonances (i.e., *2R,4S,R*<sup>Mosher</sup> and *2S,4R,R*<sup>Mosher</sup>).

While the enantiomeric pairs are readily distinguished on the basis of their integrated ratios, their relative chemical shifts and their appearance in the <sup>19</sup>F NMR spectrum reveal a striking pattern for the four resonances. Namely, one of the sets of resonances appeared as two sharp upfield signals (in a 3.5:1 integrated ratio for the *cis* and *trans* isomers), and the other set of the two <sup>19</sup>F NMR resonances (which also integrate 3.5:1) was broad and shifted downfield. Note that <sup>19</sup>F NMR spectra were broad for samples acquired in chloroform-*d*<sub>1</sub> at room temperature, and these signals are only resolved at elevated temperature (i.e., these 2-methyl pyrrolidine Mosher amides are fluxional). Similar temperature dependence and broad vs sharp signals are observed in Mosher amide derivatives of chiral 2-methyl pyrrolidines with only the C2 stereocenter (e.g., the products in Figure 1). On the basis of these observations, we attribute the features in the <sup>19</sup>F NMR spectra of the mixture of four diastereomers to an effect of the absolute configuration of the C2-stereocenter in the Mosher amide of **2b**.

As noted above, enantioselective cyclization of **2a** using {*S*-**1**}Zr(NMe<sub>2</sub>)<sub>2</sub> as the catalyst provides a 3.3:1 ratio of *cis* and *trans* diastereomers, as determined by integration of the <sup>1</sup>H NMR spectrum of the product mixture. The mixture of Mosher amide derivatives produces a <sup>19</sup>F NMR spectrum with four signals; however, the intensity of both broad downfield peaks is significantly reduced with respect to the upfield resonances.

From these experiments, the % ee values for both diastereomers are 96% (Table 1). The absolute configuration of the favored *cis* diastereomer was assigned as *2R,4R* based on the relative positions and peak shape of <sup>19</sup>F NMR signals for Mosher amides, comparisons to known configurations of 2-methylpyrrolidines, and the consistent formation of *2R* stereocenters in pyrrolidines obtained from hydroamination/cyclization when {*S*-**1**}Zr(NMe<sub>2</sub>)<sub>2</sub> is the catalyst.<sup>7,20,30</sup> Accordingly, the absolute configuration of the favored *trans* diastereomer is *2R,4S*. Note that the favored configuration of the C2 stereocenter, resulting directly from C–N bond formation, is *R* regardless of the configuration of the C4 stereocenter. Thus, the *R* configuration of the C2 stereogenic center is entirely controlled by substrate-catalyst interactions.<sup>31</sup> In contrast, it seems that the ancillary ligand exerts less influence over the C4-stereocenter that is generated by the substrate desymmetrization because the *cis* diastereomer is favored for both the achiral and the optically active catalysts.

The influence of the C2 stereocenter on the desymmetrization is probed through the variation of the R group in the prochiral substrate H<sub>2</sub>NCH<sub>2</sub>CR(CH<sub>2</sub>CH=CH<sub>2</sub>)<sub>2</sub> (compare

entries 1, 7, and 10 in Table 1 where the catalysis is performed under otherwise equivalent conditions). Here, the larger phenyl (**2a**) and *para*-bromophenyl (**4a**) groups provide higher diastereoselectivity than the smaller methyl group (**3a**). In addition, we note that the *cis* configuration is favored for both *2R* and *2S* sets of products for substrates **2a**, **3a**, and **4a**. This analysis is complicated, however, by the observation that the internal alkene substrate **6a** that affords the bulkier 2-ethylpyrrolidine product gives poorer diastereoselectivity under equivalent conditions (cf. entries 1 and 14, Table 1).

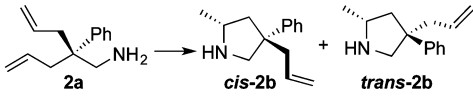

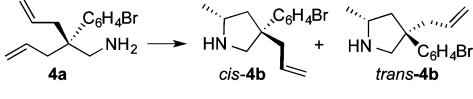
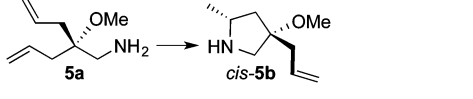

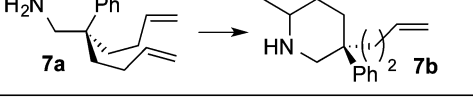
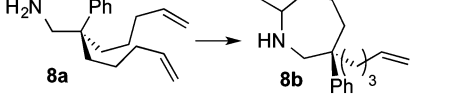
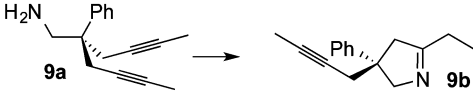
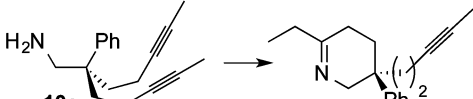
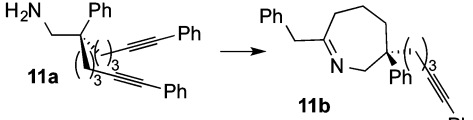
The previously reported cyclization of racemic 2-aminohex-5-ene, which contains an  $\alpha$ -methyl substituent, to a mixture of *cis* and *trans* diastereomers by achiral organolanthanides provides an interesting comparison to the present system.<sup>32</sup> In that case, the peripheral stereocenter in the substrate is fixed as either *R* or *S*, and the insipid stereocenter's configuration forms to give either *cis* or *trans* diastereomers as a racemic mixture. Notably, the diastereoselectivity of cyclization of racemic 2-aminoalkenes is affected by reaction conditions including temperature, primary amine concentration, and N-deuteration of substrate. In contrast, the stereoselectivity of cyclization of racemic 2-methyl-1-aminopent-4-ene to 2,4-dimethylpyrrolidine is insensitive to the effects of conditions, and different catalysts give a similar 60:40 ratio of diastereomers.<sup>32</sup> Although the fixed stereocenters in these two substrates should influence the ratio of diastereomers obtained, clearly the nature of the interactions vary depending on the relative positions of the stereocenters. Kinetic effects are important, but the effects are mechanistically complicated and may involve reversible coordination of chiral substrates to the organolanthanide to give diastereomeric mixtures of catalytic sites that have inequivalent reactivity and selectivity.

Previously, we observed that enantioselective cyclizations of prochiral monoalkene amines with catalytic {*S*-**1**}Zr(NMe<sub>2</sub>)<sub>2</sub> (e.g., the reaction of Figure 1) also show some of these effects.<sup>20</sup> In particular, substrate N-deuteration increases the % ee of the pyrrolidine product, as does lower reaction temperatures. However, the reaction concentration does not affect the enantiomeric ratio of the products.

We were curious about the effects of these parameters (isotopic perturbation of stereochemistry, concentration, and temperature) on the cyclization of aminodialkenes because an interesting opportunity arises with respect to the achiral organolanthanide-catalyzed cyclization of racemic aminoalkenes. In the asymmetric hydroamination/desymmetrization system, the C2 stereocenter is established through ligand-controlled stereoselectivity, but it is also formed concurrently with respect to the stereocenter generated by desymmetrization. That is, coordination of multiple prochiral substrates to a single zirconium center does not generate diastereomeric catalytic sites (although catalyst speciation may be affected by the number of coordinated substrates).

Thus, we investigated the effects of concentration, primary and secondary amine additives, and temperature as a rational strategy for controlling the diastereoselectivity of {*S*-**1**}Zr(NMe<sub>2</sub>)<sub>2</sub>-catalyzed cyclization of **2a** to **2b** in toluene. Note that catalyst and substrate concentration have quantitative kinetic implications that can inform upon mechanism, as opposed to the catalyst:substrate ratio (aka, catalyst loading) which reports on catalytic efficiency. The first part of this study was accomplished experimentally by increasing the total volume of reaction mixture by adding solvent. The catalyst loading relative to substrate was kept constant (10 mol %); however,

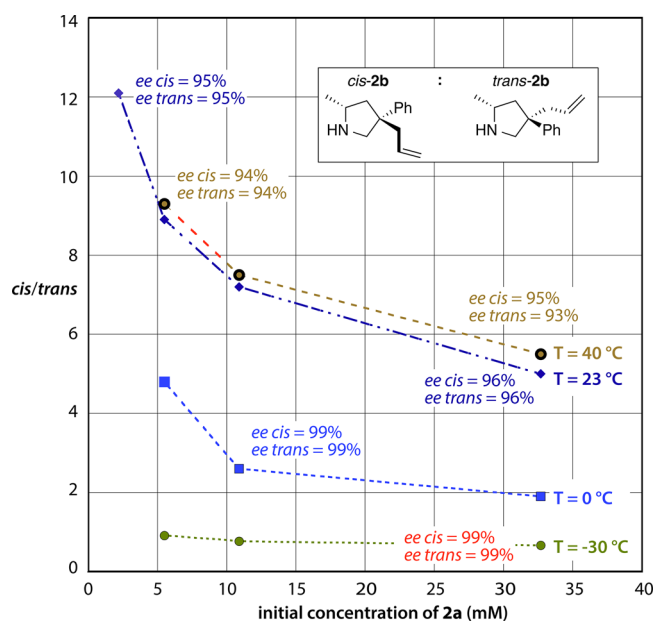
Table 1. Diastereoselective and Enantioselective Cyclization of Aminodialkenes and Aminodialkynes Catalyzed by  $\{S-1\}Zr(NMe_2)_2$ <sup>a</sup>

| Reaction  | Entry | [Substrate]          | Time  | Yield (%) <sup>b</sup> | <i>cis:trans</i> <sup>c</sup> | % ee <sup>c</sup>     |
|---|-------|----------------------|-------|------------------------|-------------------------------|-----------------------|
| <br>$2a \rightarrow cis-2b + trans-2b$ | 1     | 65.4 mM              | 0.5 h | 100 (96)               | 3.3:1                         | 96, 96                |
|   | 2     | 5.45 mM              | 6 h   | 100 (94)               | 8.9:1                         | 96, 95                |
|   | 3     | 65.4 mM <sup>d</sup> | 55 h  | 100                    | 1.96:1                        | 96, 96                |
|   | 4     | 5.45 mM              | 4 d   | 95 <sup>e</sup>        | 1:1.1                         | 99, 99 <sup>f</sup>   |
|   | 5     | 327 mM               | 4 d   | 95 <sup>e</sup>        | 1:4.5                         | 99, 99                |
|   | 6     | 327 mM <sup>g</sup>  | 6 d   | 100 (93) <sup>e</sup>  | 1:6                           | 99, 99                |
| <br>$3a \rightarrow cis-3b + trans-3b$ | 7     | 65.4 mM              | 0.5 h | 100 (92)               | 1:1.1                         | 93, 92                |
|   | 8     | 5.45 mM              | 2 d   | 100 (84)               | 4.2:1                         | 93, 92                |
|   | 9     | 327 mM <sup>g</sup>  | 6 d   | 100 (90) <sup>e</sup>  | 1:6.5                         | 96, 97                |
| <br>$4a \rightarrow cis-4b + trans-4b$ | 10    | 65.4 mM              | 0.5 h | 100 (94)               | 4:1                           | 97, 95                |
|   | 11    | 5.45 mM              | 3 h   | 100 (95)               | 8:1                           | 95 ( <i>cis</i> )     |
| <br>$5a \rightarrow cis-5b$            | 12    | 327 mM               | 48 h  | 90                     | 10:1                          | 97 ( <i>cis</i> )     |
|   | 13    | 65.4 mM              | 48 h  | 90 (78)                | >20:1                         | 97 ( <i>cis</i> )     |
| <br>$6a \rightarrow cis-6b$           | 14    | 65.4 mM              | 4 d   | 87 (78)                | 2:1                           | 93, 95                |
|   | 15    | 10.9 mM              | 8 d   | 81 (75)                | 8:1                           | 92 ( <i>cis</i> )     |
| <br>$7a \rightarrow 7b$              | 16    | 65.4 mM              | 3 d   | 90 (82)                | 2.4:1                         | 33, 12 <sup>f,h</sup> |
|   | 17    | 5.45 mM              | 4 d   | 85 (76)                | 6.6:1                         | 32, 12 <sup>f,h</sup> |
| <br>$8a \rightarrow 8b$              | 18    | 65.4 mM              | 4 d   | 90                     | 2.8:1                         | 89, 92 <sup>h</sup>   |
|   | 19    | 16.4 mM              | 6 d   | 86 (74)                | 7:1                           | 89, 91 <sup>h</sup>   |
| <br>$9a \rightarrow 9b$              | 20    | 65.4 mM              | 0.6 h | 100 (95)               | n.a.                          | 87 <sup>f,h</sup>     |
|   | 21    | 5.45 mM              | 2 h   | 100 (95)               | n.a.                          | 91 <sup>f,h</sup>     |
| <br>$10a \rightarrow 10b$            | 22    | 65.4 mM              | 20 h  | 100 (93)               | n.a.                          | 71 <sup>f,h</sup>     |
|   | 23    | 5.45 mM              | 48 h  | 100 (94)               | n.a.                          | 77 <sup>f,h</sup>     |
| <br>$11a \rightarrow 11b$            | 24    | 5.45 mM              | 72 h  | 100 (89)               | n.a.                          | 89 <sup>f,h</sup>     |

<sup>a</sup>10 mol %  $\{S-1\}Zr(NMe_2)_2$ , room temperature. <sup>b</sup>Isolated yield. <sup>c</sup>The *cis:trans* ratios and % ee (*cis*, *trans*) were determined by <sup>1</sup>H and/or <sup>19</sup>F NMR spectra of Mosher amide derivatives. <sup>d</sup>Amyl amine (29 mM). <sup>e</sup>-30 °C. <sup>f</sup>The % ee values were verified by HPLC. <sup>g</sup>Propyl amine (100 mM). <sup>h</sup>Absolute stereochemistry was not assigned.

the absolute substrate and catalyst concentration decreased in these experiments with a systematic increase in solvent volume. Interestingly, *cis-2b* is increasingly and systematically favored over *trans-2b* upon dilution of the reaction medium. For example, the *cis/trans* ratio increased from 3.3:1 to 9:1 by diluting the reaction mixture 12-fold and then to 12:1 after a 30-fold dilution. This effect is illustrated in Figure 4, which

plots the *cis/trans* ratio vs reaction concentration. The *cis* isomer is systematically favored under more dilute reaction conditions (on the left side of the plot). In contrast, the % ee values for the two diastereomers are barely changed in these experiments. Using the room-temperature data to illustrate the stability of the C2 stereocenter, (the data illustrated with diamond symbols in Figure 4 and entries 1 and 2 in Table 1),

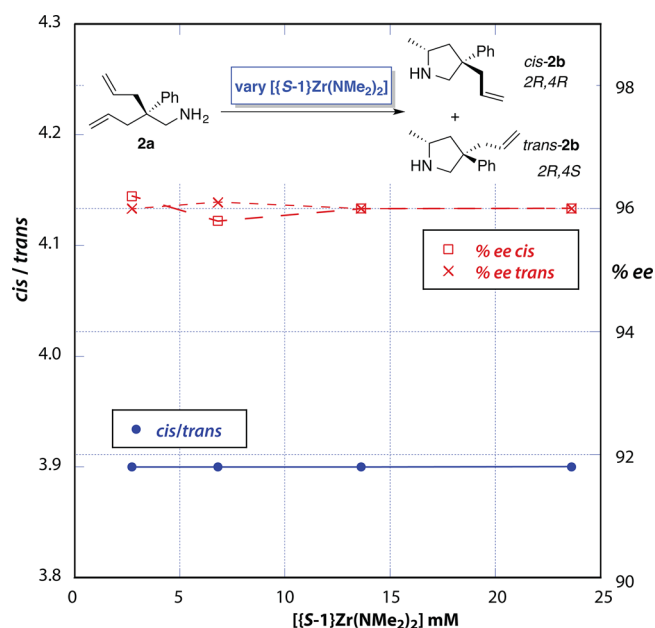


**Figure 4.** Plots of the *cis/trans* ratio (*cis-2b/trans-2b*) vs concentration of the reaction mixture (defined by  $[2a]_{ini}$ ). Each point is a separate experiment, and each curve shows a set of reactions performed at a single temperature (black open circles, 40 °C; blue diamonds, 23 °C; blue solid squares, 0 °C; olive green solid circles, -30 °C). For each data point, the catalytic experiment was performed with 10 mol %  $\{S-1\}Zr(NMe_2)_2$  in toluene. The lines connecting the points are added to help visualize the data.

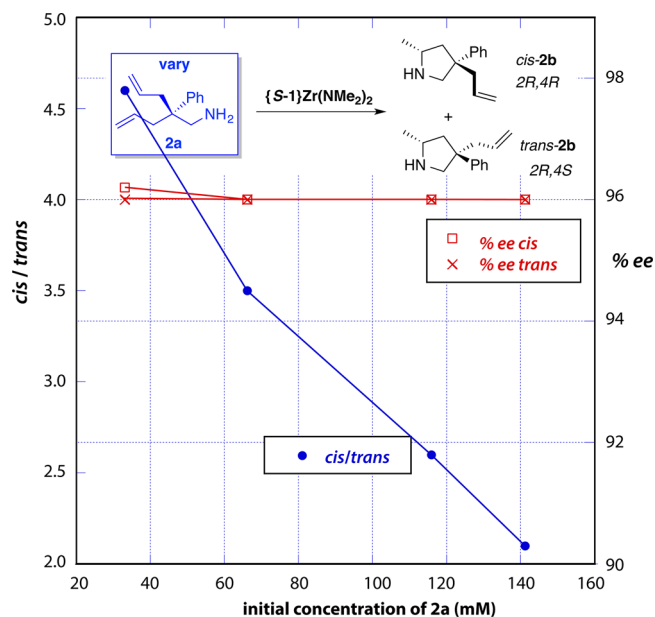
the enantiomeric excesses for *cis* and *trans* diastereomers are ca. 95–96% for experiments performed at 65 mM and at 2.25 mM even while the *cis/trans* ratio varies from 3.3:1 to 12:1. In addition, the reaction rate decreases at lower concentrations. A straightforward analysis of the experimental rate law  $-d[2a]/dt = k_{obs}[Zr]^1[2a]^1$  predicts this effect (see below). A similar *cis/trans* ratio is obtained in benzene, although the systematic effect of solvent on diastereoselectivity is not yet explored.

The effect of temperature on the *cis/trans* ratio is also illustrated in the plot of Figure 4, which shows that the *cis* isomer is increasingly favored as the temperature increases. The enantioselectivities for the *cis* (defined by  $(RR-SS)/(RR+SS)$ ) and *trans* diastereomers  $(RS-SR)/(RS+SR)$  decrease slightly as the temperature increases. Thus, the rate of formation of the *SS* isomer increases at higher temperature with respect to the less favored *RS/SR* isomers. The *RR* isomer is still the major product. Conversely, the *trans* diastereomer is favored at low temperature (-30 °C). This effect can be combined with the effect of concentration (*trans* is favored at high concentration) to impressively flip the diastereoselectivity from *cis:trans* = 12:1 to favor the *trans* over the *cis* isomer by 1:4.5 while maintaining enantioselectivities >95%.

The catalyst and substrate concentrations were simultaneously varied in the above experiments, so the next set of experiments were designed to decouple these two variables (Figures 5 and 6). Variation of catalyst concentration from 13.6 to 2.7 mM while maintaining a constant initial concentration of substrate does not affect the *cis:trans* ratio which is consistently 3.9:1 at full conversion ( $[2a]_{ini} = 52$  mM, Figure 5). In these experiments, the catalyst:substrate ratio changes for each data point because the initial substrates' concentrations are invariant over the four experiments. These data clearly show that both %



**Figure 5.** Plot of the *cis:trans* ratio for **2b** obtained from cyclization of **2a** as the concentration of the catalyst  $\{S-1\}Zr(NMe_2)_2$  is varied and the initial substrate concentration  $[2a]_{ini}$  is held constant between experiments at 52 mM. The left y-axis reports the *cis/trans* ratio (data points identified by blue solid circles), while the right y-axis shows the % ee for the products (data points identified by red open squares for % ee *trans* and red "x" for % ee *cis*).



**Figure 6.** Plot of the *cis:trans* ratio for **2b** obtained from cyclization of **2a** as the initial concentration of **2a** is varied, and the concentration of catalyst is held constant. The left y-axis reports the *cis/trans* ratio (data points identified by blue solid circles), while the right y-axis shows the % ee for the products (data points identified by red open squares for % ee *trans* and red "x" for % ee *cis*).

ee and the diastereoselectivity are not affected by catalyst loading or catalyst concentration.

Remarkably and in contrast to the interpretation of the data in Figure 5, the *cis* isomer is increasingly favored as the initial substrate concentration decreases from 116 to 31 mM, while

the catalyst concentration is kept constant ( $[\{S-1\}Zr(NMe_2)_2] = 6.5 \text{ mM}$ , Figure 6).

The % ee for both diastereomers is unaffected by these changes in reaction condition (96% and 96%, respectively). Together, these experiments indicate that the effects of reaction conditions on diastereoselectivity are best evaluated in the context of substrate concentration rather than catalyst concentration or catalyst loading.

A possible rationalization of these effects involves coordination of substrate **2a** and/or product **2b** to the catalytic site to affect the reaction's diastereoselectivity, and we sought to differentiate these possible effects to further clarify the factors that influence the pyrrolidine products' *cis:trans* ratio. To accomplish this, the cyclization of **2a** was performed in the presence of 5 equiv of the product **R-2b** (*cis:trans* = 3.3:1) or its enantiomer **S-2b** (3.3:1). Both experiments give the product with a *cis:trans* ratio of 3.3:1. This ratio is the same as obtained in the absence of additional product (Table 1, entry 1), although the reaction time is increased approximately 50× with 5 equiv of **2b** compared to additive-free conditions.

Thus, high substrate concentration and low reaction temperatures favor the *trans* diastereomer. This selectivity can be further improved by addition of primary amines such as propylamine or amylamine; however, the reaction times are increased in the presence of amine additives. Note that both pyrrolidine product and propylamine additives decrease the reaction rate, but only the primary amine affects the *cis:trans* ratio. This is demonstrated in two examples in Table 1. Under moderately *cis*-selective conditions (room temperature, 65.4 mM), the addition of amylamine decreases the *cis:trans* ratio from 3.3:1 to 1.96:1 (entries 1 and 3). Under *trans*-selective conditions ( $-30 \text{ }^\circ\text{C}$ , 327 mM), the addition of propylamine increasingly favors the *trans* isomer. This effect is highlighted by comparison of entries 5 and 6, in which the *cis:trans* ratio goes from 1:4.5 to 1:6 upon addition of propylamine.

The influence of concentration, primary amine additive, and temperature may be used to tune the asymmetric catalytic reaction for either diastereomer (Table 1). In particular, high concentration of substrate **2a**, propylamine additive, and a reaction temperature of  $-30 \text{ }^\circ\text{C}$  gives the *trans* (*2R,4S*, major isomer) diastereomer favored over *cis* (*2R,4R*, major isomer) in a 6:1 ratio. The enantiomeric excess for both diastereomers under these conditions is 99%. In contrast, high temperature and dilute conditions favor the *cis* isomer. Thus, the reaction conditions allow the C4 stereocenter of pyrrolidine **2b** to switch from favoring *S* to favoring *R* with a single catalyst.

The series of diallyl amine substrates of Table 1 were used to begin to probe the generality of the effects of reaction conditions on the enantioselectivity and diastereoselectivity of  $\{S-1\}Zr(NMe_2)_2$ -catalyzed cyclization and desymmetrization. In general, both *cis* and *trans* pyrrolidine products are obtained with excellent enantiomeric excesses. As described in detail for substrate **2a**, dilute conditions generally favor the 2-methyl and bulkier 4-substituent in mutual *cis* disposition (putting the 2-methyl and 4-allyl group *trans*). In the special case of 4-allyl-2,4-dimethylpyrrolidine (**3b**) and in contrast to products **2b**, **4b**, and **5b**, the *cis-3b* isomer places the 2-methyl and 4-allyl on the same face of the compound. Despite this change in assignment with respect to 2-methyl/4-allyl disposition, the diastereoselective cyclization follows the same pattern as observed for **2a**, **4a**, and **5a**. Thus, the *trans* product is favored over the *cis* by 6.5:1 at  $-30 \text{ }^\circ\text{C}$  under concentrated conditions (327 mM **3a**) with propylamine (100 mM) as an additive, whereas dilute

conditions favor the *cis* isomer 4.2:1. Analysis of the series of favored diastereomers for products **2b**, **3b**, **4b**, and **5b** suggests that the products are obtained at higher temperature and dilute conditions through a stereochemistry-determining step that places the bulkier group *cis* to the insipient 2-methyl moiety.

As noted previously, the catalyst derived from  $\{S-1\}Zr(NMe_2)_2$  is active for hydroamination in the presence of ether and aryl bromide functionalities.<sup>20</sup> Notably, 4-allyl-4-methoxy-2-methylpyrrolidine (**5b**) is obtained upon cyclization of **5a** essentially as a single isomer (*2R,4S*) with 2-methyl and 4-methoxy groups disposed *cis*. The assignment of the major isomer as *cis-5b* is supported by NOE experiments in benzene- $d_6$  in which irradiation of the 2H signal of the major isomer (3.26 ppm) results in decreased intensity of the olefin resonances at 5.86 and 5.04 ppm. In addition, cyclization involving an internal alkene in substrate **6a** increasingly favors *cis*-disposed ethyl and phenyl groups under dilute conditions, again with high enantioselectivity (Table 1, entries 14 and 15).

The effect of substrate concentration on the desymmetrization of the prochiral quaternary center extends to the cyclizations that give 2-methylpiperidines and 2-methylazepanes as mixtures of enantiomeric pairs of diastereomers. Previously, we reported that the catalyst generated from  $\{S-1\}Zr(NMe_2)_2$  is less enantioselective and less active for the formation of 2-methyl-5,5-disubstituted-piperidines than 2-methyl-4,4-disubstituted-pyrrolidines.<sup>20</sup> Despite this limitation which means that both *2S* and *2R* stereocenters are abundant in the product **7b**, dilute conditions provide a d.r. of 6.6:1. The catalyst is more effective for azepane formation, and the cyclization of **8a** gives improved diastereoselectivity for the *cis* product (verified by NOE between Ph and Me groups) with the dilute reaction conditions. Azepane **8b** is produced with impressive enantioselectivity for seven-membered ring formation (Table 1, entries 18 and 19). Note that more concentrated conditions result in poorer diastereoselectivity in the desymmetrization reactions that give the piperidine and azepane products, following the trends established for pyrrolidines. In these systems, as for the *cis* and *trans* pyrrolidines, the % ee values for both *cis* and *trans* diastereomers are barely changed between concentrated and dilute conditions.

The hydroamination/cyclization/desymmetrization of dialkynylamines provide an opportunity to further decouple the C2 and C4 stereocenters by eliminating the former. In addition, the breadth of the synthetic method is expanded in aminoalkyne cyclizations through the formation of an optically enriched product that may be further derivatized at imine and alkyne functional groups. Cyclization of substrates **9a-11a** provides 1,2-didehydropyrrolidine (**9b**), 1,2-didehydropiperidine (**10b**), and 1,2-didehydroazepane (**11b**) products in excellent yield and promising enantioselectivity (up to 91%). As in the desymmetrization of nonconjugated dienes, dilute conditions increase selectivity for the major isomer. Because the cyclization reaction provides enantioenriched product and no other stereocenters are present, the enantioselectivity of the desymmetrization reaction must be controlled by the chiral catalytic site.

Furthermore, the 77% ee obtained for the six-membered ring **10b** corresponds to a ratio of enantiomers (e.r.) of 7.7:1, which is slightly higher than the ratio of diastereomers for piperidine **7b** obtained from the dialkynylamine **7a** under similar reaction conditions. Under more concentrated conditions, an e.r. of 5.9:1 is obtained for **10b** (71% ee). The effect of concentration

on the desymmetrization of dialkynylamines is less influential than in the conversion of dialkenylamines, but it is sufficient to impact synthetic protocols. The enantioenriched nitrogen heterocycles bearing quaternary stereocenters<sup>9</sup> are difficult to prepare in enantioenriched form by other methods, although their importance is highlighted by the synthesis of target compounds such as (+)-vincamine, madindolines A and B,<sup>19</sup> quadrigemine C, and conessine.<sup>33,34</sup>

Catalytic rates of N-deuterium-enriched aminoalkene cyclizations are slower than corresponding naturally abundant isotopomers; however, the effect of N-deuteration on stereoselectivity varies case-to-case. In  $(C_5Me_5)_2LnCH(SiMe_3)_2$ -catalyzed cyclizations of racemic aminoalkenes, 2,5-dimethylpyrrolidine is formed with *trans* selectivity (up to 50:1 in the presence of propylamine), whereas 2,5-dimethylpyrrolidine-*d*<sub>2</sub> forms with a 1:1 *cis:trans* ratio.<sup>32</sup> In contrast,  $\{S-1\}Zr(NMe_2)_2$  catalyzes aminoalkene cyclizations with improved enantioselectivity upon isotopic substitution, and this effect provided a key data point for a proposed six-atom center, two-substrate transition state for C–N bond formation (Figure 1).<sup>20</sup>

Therefore, isotope effects on rate and isotopic perturbations of the diastereoselectivity and enantioselectivity were investigated in the present aminodialkene and aminodialkyne systems. As in our previous kinetic studies, the experimental second-order rate laws in eqs 1 and 2 exhibit concentration dependencies on precatalyst and substrate for reactions of aminodialkene **2a** or aminodialkyne **9a** ( $k_{obs}^{(2a)} = 0.14(1) M^{-1} s^{-1}$  at 23 °C;  $k_{obs}^{(9a)} = 0.17(3) M^{-1} s^{-1}$  at 23 °C).

$$-\frac{d[2a]}{dt} = k_{obs}^{2a}[2a]^1[\{S-1\}Zr(NMe_2)_2]^1 \quad (1)$$

$$-\frac{d[9a]}{dt} = k_{obs}^{9a}[9a]^1[\{S-1\}Zr(NMe_2)_2]^1 \quad (2)$$

The rate laws were determined with 5.7–16.4 mM  $[\{S-1\}Zr(NMe_2)_2]$  and 0.13–0.14 M  $[2a]_{ini}$  or 0.17–0.19 M  $[9a]_{ini}$ , giving *cis/trans* ratios for **2b** from 2.5:1 to 2.6:1. The rate constant for cyclization/desymmetrization of dialkynylamine **9a** is slightly larger than that of the aminodialkene **2a**.

For comparison, the second-order rate constant for cyclization of the monoalkenylamine C-(1-allyl-cyclohexyl)-methylamine by  $\{S-1\}Zr(NMe_2)_2$  is 0.128(7)  $M^{-1} s^{-1}$ .<sup>20</sup> Thus, the cyclization of this dialkenyl substrate is slightly faster than the monoalkenyl substrate. We had previously shown that the second-order rate law for cyclization of aminoalkenes masks significantly more complex kinetic behavior that includes a reversible substrate–catalyst binding (assigned based on saturation observed in initial rates plots) and catalytic inhibition at high substrate concentration. The former observation was interpreted to rule out protonolysis as the turnover-limiting step of the catalytic cycle. The similarity of the overall second-order rate law for  $\{S-1\}Zr(NMe_2)_2$ -catalyzed cyclization of C-(1-allyl-cyclohexyl)-methylamine, **2a**, and **9a** suggests that closely related pathways are operative in all three cases. Additional parallel observations related to isotope effects (described below), stereochemistry and absolute configuration described above, further support the idea that the pathway for this zirconium-catalyzed cyclization of aminoalkenes, aminodialkenes, and aminodialkynes is closely related.

Catalytic conversion of the N-labeled substrate **9a-d**<sub>2</sub> follows the above rate law, but the conversion is noticeably slower than the reaction of **9a** ( $k_{obs}^{(9a-d_2)} = 0.042(2) M^{-1} s^{-1}$ ). The  $k_H/k_D$  value of 4.1(7) is consistent with a primary kinetic isotope

effect and suggests that an N–H bond is broken during the turnover-limiting step in the catalytic conversion of **9a** under the conditions of the kinetic measurements. An alternative interpretation of the isotope effect invokes reversible hydrogen transfer to a lower energy oscillator (an equilibrium isotope effect)<sup>35,36</sup> prior to the irreversible, turnover-limiting step that does not necessarily involve a proton transfer. The compounds  $HNMe_2$  and **2b** or **9b** are formed within 30 s of mixing substrate and precatalyst, suggesting a fast exchange of amine/amide; however, this exchange is unlikely to provide a large equilibrium isotope effect because both oscillators are N–H bonds. Unfortunately, the catalyst resting state, which is the species that likely would participate in the equilibrium, was not detected through *in situ* <sup>1</sup>H NMR spectroscopic studies, even at low temperature.

Deuterium isotope effects on catalytic diastereoselectivity and enantioselectivity probe the relationship between the turnover-limiting step, the C–N bond forming step which establishes the C2 stereocenter, and the desymmetrization of the prochiral C4 quaternary center (Table 2). The experiments reveal that ND substitution influences the stereoselectivity at both stereocenters, as demonstrated by cyclizations of **2a** vs **2a-d**<sub>2</sub> and **3a** vs **3a-d**<sub>2</sub> (Table 2).

In a dramatic example, the *cis:trans* ratio of **2b** increases from 8:1 to 31:1 for **2b-d**<sub>2</sub>, and the optical purity of *cis-2b-d*<sub>2</sub> improves to 99%. In addition, the enantiotopic catalyst  $\{R-1\}Zr(NMe_2)_2$  catalyzes the cyclization of **2a-d**<sub>2</sub> to *cis-2S,4S-2b-d*<sub>2</sub>, which is the expected enantiomer.

In addition, desymmetrization reactions of N-deuterium-labeled dialkynylamines occur with greater enantioselectivity than those of the corresponding unlabeled substrates. Thus, the C5-chiral 1,2-dehydropiperidine is prepared with enantiomeric excess up to 81% through a catalytic asymmetric hydroamination reaction.

Finally, a startling disconnect between enantioselectivity and diastereoselectivity is evident from plots of the % ee and *cis:trans* ratio as a function of conversion (Figure 7). The enantioselectivity (plotted on the right y-axis) is constant up to ca. 80% conversion, at which point there is an abrupt change in % ee. The reaction was performed at 10 mol %  $\{S-1\}Zr(NMe_2)_2$ , and 80% conversion means that only 2 equiv of **2a** remains in the reaction mixture at that point. This sharp drop had been previously observed in the  $\{S-1\}Zr(NMe_2)_2$ -catalyzed cyclization of aminoalkenes, and we suggested a change in mechanism occurs when the substrate/catalyst ratio drops below 2.<sup>20</sup>

In contrast, the *cis:trans* ratio improves in a near-linear fashion as conversion increases (plotted on the left y-axis in Figure 7). This trend is likely related directly to the effect of substrate concentration on diastereoselectivity; as the reaction proceeds, the concentration of the primary aminodialkene decreases and the *cis:trans* ratio increases. This experiment shows that the diastereoselectivity observed at the conclusion of the cyclization reactions is the result of an average of the substrate concentration over the course of the reaction. These two observations can be rationalized by two highly enantioselective and rapidly equilibrating catalytic sites; the ratios of these sites change as a function of substrate concentration (resulting from catalytic conversion) as illustrated in Figure 8.

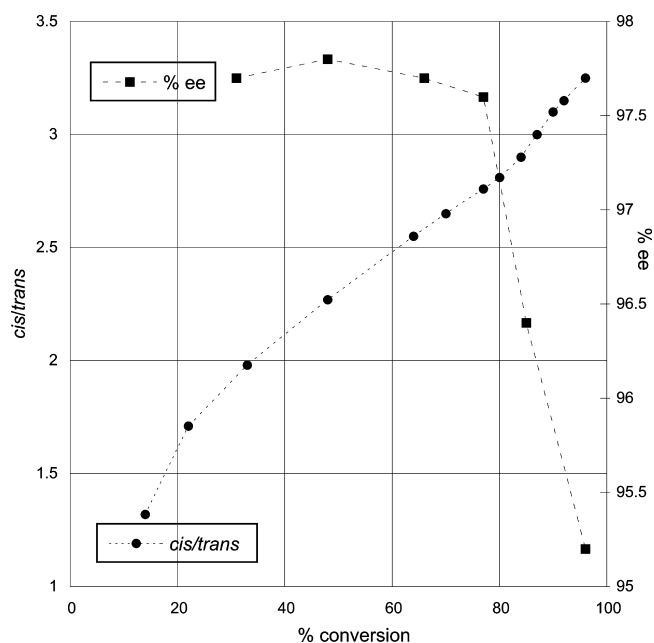
Given that the diastereoselectivity is affected by  $RNH_2$  concentration, we propose that the *cis*-selective catalytic site is  $\{S-1\}Zr(NHR)_2$  and the *trans*-selective site is the primary

**Table 2.** *Cis:trans* and % ee Values for Natural Abundance and Deuterium-Labeled Hydroamination Products From {*S*-1}Zr(NMe<sub>2</sub>)<sub>2</sub>-Catalyzed Cyclization/Desymmetrization<sup>a</sup>

| Reaction | <i>cis:trans</i> <sup>b</sup> | % ee <sup>c</sup>                 |
|----------|-------------------------------|-----------------------------------|
|          | 8:1                           | 96, 95<br>( <i>cis, trans</i> )   |
|          | 31:1 <sup>d</sup>             | 99 ( <i>cis</i> ) <sup>e</sup>    |
|          | 43:1 <sup>d</sup>             | 97 <sup>f</sup><br>( <i>cis</i> ) |
|          | 4.2:1                         | 93, 92<br>( <i>cis, trans</i> )   |
|          | 5.3:1                         | 98, 95<br>( <i>cis, trans</i> )   |
|          | n.a.                          | 91% <sup>g</sup>                  |
|          | n.a.                          | 93% <sup>g</sup>                  |
|          | n.a.                          | 77% <sup>g</sup>                  |
|          | n.a.                          | 81% <sup>g</sup>                  |

<sup>a</sup>Reaction conditions: 10 mol % catalyst [{*S*-1}Zr(NMe<sub>2</sub>)<sub>2</sub>] = 0.545 mM, room temperature, [substrate] = 5.45 mM. <sup>b</sup>The *cis:trans* ratios were determined by <sup>19</sup>F NMR spectra of Mosher amide derivatives. <sup>c</sup>The % ee values were determined by <sup>19</sup>F NMR spectra of Mosher amide derivatives. <sup>d</sup>The *cis:trans* ratio was determined by HPLC. <sup>e</sup>The % ee was evaluated by HPLC. <sup>f</sup>[[*R*-1}Zr(NMe<sub>2</sub>)<sub>2</sub>] = 0.41 mM was used as the catalyst, [2a-d<sub>2</sub>] = 4.1 mM. <sup>g</sup>Absolute stereochemistry was not assigned.

amine adduct {*S*-1}Zr(NHR)<sub>2</sub>(NH<sub>2</sub>R) (R = unsaturated hydrocarbyl). We suggest that unfavorable steric interactions between the coordinated amine and the cyclizing aminoalkene give a ring conformation with the smaller substituent axial, yet away from the coordinated amine. The favored location of the bulkier substituent is equatorial, giving a *trans* configuration. In the amine-free catalytic site, the bulkier group may be *cis*, as the incipient ring conformation and {*S*-1} ancillary allows the allyl group to be axial and pointed away from the cyclopentadienyl ring. As the primary amine concentration is reduced throughout the conversion, the relative percentage of {*S*-1}Zr(NHR)<sub>2</sub> increases with respect to the amine adduct resulting in the observed linear increase in *cis:trans* product ratio. The isotope effect on diastereoselectivity is consistent with this interpretation, because possible adduct structures involving amine coordination or a hydrogen-bonding interaction would reduce the NH oscillator energy and be less favored for the heavier isotope. As a result, the deuterated substrate would favor the *cis*-selective catalyst. In contrast, the % ee of 2b is essentially constant for approximately 80% of the conversion and sharply



**Figure 7.** *Cis:trans* ratio and % ee of hydroamination product 2b as a function of catalytic conversion. Diastereoselectivity is plotted on the left y-axis with (●), while the % ee is plotted on the right y-axis with (■). Reaction conditions: 10 mol % catalyst [{*S*-1}Zr(NMe<sub>2</sub>)<sub>2</sub>] = 6.81 mM, [2a] = 68.1 mM, benzene, room temperature.

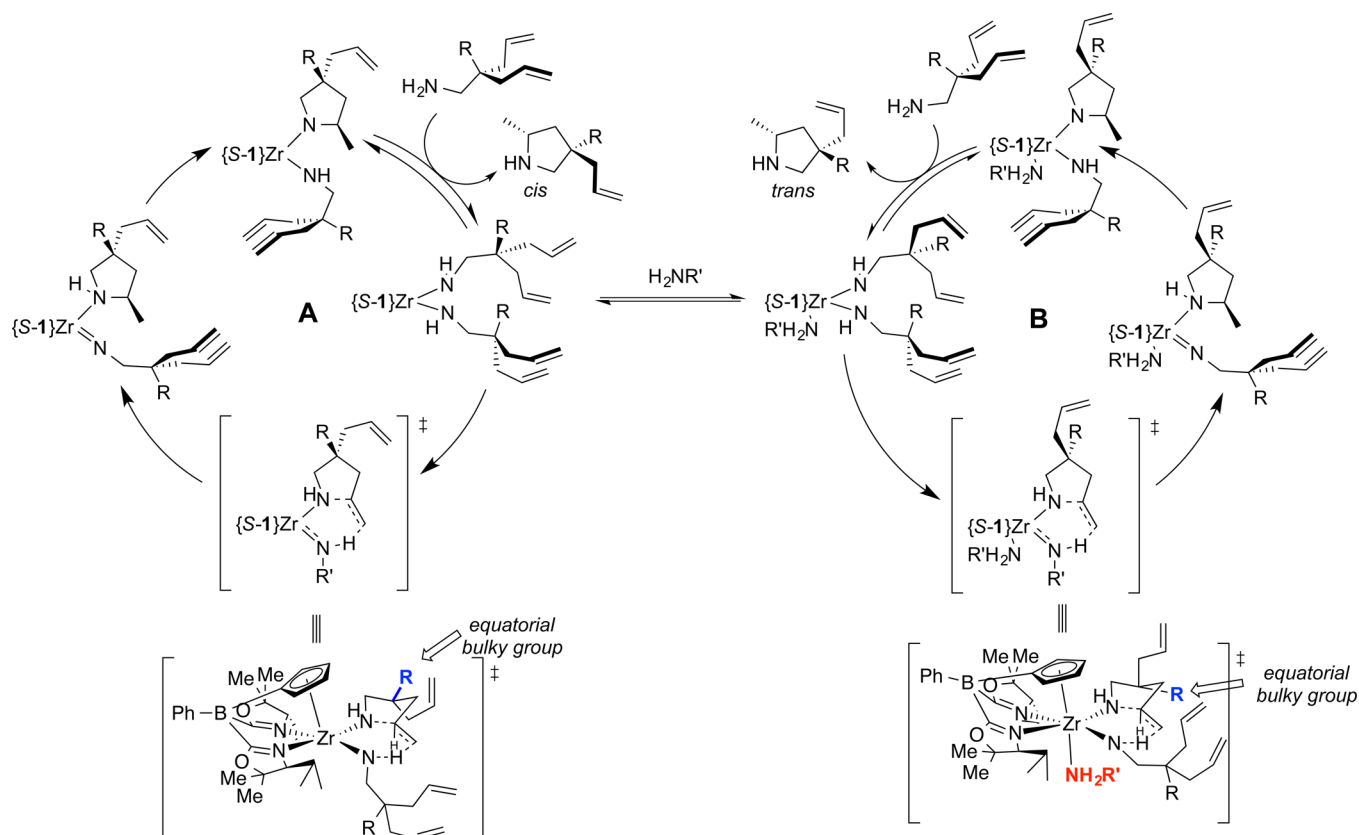
drops when the catalyst:substrate ratio approaches 1:2; a similar effect observed for aminoalkenes was attributed to a change in the C–N bond forming mechanism.<sup>20</sup> Remarkably, this interpretation suggests that two forms of the catalyst react with the same enantiotopic preference and a third catalyst species gives lower stereoselectivity only at low [primary amine]:[Zr] ratios.

In addition, the effects of primary vs secondary amine additive on rate and stereoselectivity are worth considering in the context of this model. The diastereoselectivity is influenced by primary amines, but there is no effect of secondary pyrrolidine product on diastereoselectivity. Both primary and secondary noncyclizable amines inhibit the rate of cyclization. The latter observation is consistent with both types of amine additives occupying catalytic sites as amides. For cyclization to occur, however, two primary zirconium amide sites are required. While a pyrrolidine might coordinate to zirconium(IV) as a neutral donor in the resting state of cycle B, likely exchange would provide the catalytically inactive zirconium pyrrolide species. As a result, high concentrations of pyrrolidine inhibit catalysis but do not influence the *cis/trans* product ratio. In the lower activity and lower enantioselectivity catalytic regime, the zirconium speciation likely includes coordinated pyrrolidine and pyrrolide ligands, but the role of such species in the catalytic conversion is not yet understood.

## CONCLUSION

The features of these aminodialkene and aminodialkyne cyclization and desymmetrization reactions reveal that the  $\alpha$ -amino stereocenter and the quaternary stereocenter are controlled by a series of partly overlapping variables that affect the active catalyst and the reaction mechanism. Using concentration, temperature, and isotopic substitution, a single precatalyst provides access to either *cis* or *trans* products with high optical purity, and optimized conditions provide the





**Figure 8.** A pathway that rationalizes concentration-dependent *cis/trans* selectivity with an exchanging two-site catalytic model. The configuration of the pyrrolidine product is guided by unfavorable interactions with the bulky substituent in the axial position. Coordination of amine (cycle B) changes the ring conformation to place the *cis* group axial, which would result in unfavorable steric interactions between the bulkier substituent on the cyclizing amine if the stereocenter's configuration did not flip to give the *trans* diastereomer. As the concentration of the primary amine decreases over the course of the reaction, the equilibrium between the two cycles shifts to favor cycle A.

product as a single stereoisomer. No bicyclization product was detected with these zirconium-based catalysts. All four stereoisomeric products can be prepared with this catalytic method because both  $\{S-1\}$  and  $\{R-1\}$ -based zirconium compounds are accessible. The proposed interpretation of the data is that the catalytic site is affected by substrate concentration, and the change in catalytic site influences the diastereoselectivity via the 4C stereocenter (desymmetrization). Remarkably, the apparent changes in catalyst structure do not significantly affect the enantioselectivity of the 2C stereocenter.

Furthermore, the *cis:trans* ratio is also influenced by the ancillary ligand based on comparisons between achiral  $\{\text{PhB}(\text{Ox}^{\text{Me}_2})_2\text{C}_3\text{H}_4\}\text{Zr}(\text{NMe}_2)_2$  and  $\{S-1\}\text{Zr}(\text{NMe}_2)_2$ . Thus, the ancillary ligand will provide additional parameters for tuning enantioselectivity and diastereoselectivity. A particularly interesting ligand design strategy would deliver a primary amine donor to the active site to favor the *trans* diastereomeric products. In the present system, this effect is achieved through the addition of a propylamine additive at the expense of catalytic rate. We are currently investigating these catalyst design principles to better understand the reaction mechanism and improve the synthetic application of this chemistry.

In addition, the enantioselective aminodialkynes desymmetrization reactions afford optically active 1,2-dehydropyrrolidine, piperidine, and azepane molecules. The reaction variables that influence diastereoselectivity for aminodialkene desymmetrization also influence enantioselectivity in the dialkyne desymmetrization, although to a lesser degree. Still, this method provides

synthetic flexibility resulting from the imine and alkyne functionality present in the optically enriched product.

Importantly, the effects of concentration and temperature, as well as isotopic perturbation of the hydroamination and desymmetrization-produced stereocenters, extend over five-, six-, and seven-membered rings as well as substrates containing alkenes and alkynes. That is, the effects are not specific to a single ring size or controlled by the thermodynamics favoring five-membered ring formation. As has been noted in organolanthanide-catalyzed cyclizations of aminoalkenes and aminoalkynes, the rate laws for both types of unsaturated substrates have the same form, and likely the zirconium-catalyzed pathways that give conversion are closely related to one another. With this in mind, other catalytic asymmetric desymmetrization reactions that involve additions of amines to olefins may provide valuable optically enriched amines containing peripheral stereocenters.

## EXPERIMENTAL SECTION

**General Experimental.** All reactions were performed under a nitrogen atmosphere in a glovebox under water-free and air-free conditions.  $\{\text{PhB}(\text{Ox}^{4S\text{-iPrMe}_2})_2\text{C}_3\text{H}_4\}\text{Zr}(\text{NMe}_2)_2$  ( $\{S-1\}\text{Zr}(\text{NMe}_2)_2$ ),<sup>20</sup> 2-allyl-2-(4-bromophenyl)pent-4-enylamine (**4a**),<sup>21</sup> and 2-(but-2-ynyl)-2-phenylhex-4-yn-1-amine (**9a**)<sup>37</sup> were prepared by published procedures, and their catalytic cyclizations to give **4b** and **9b** are given as representative examples. Full experimental details for synthesis, characterization, and cyclization of all substrates are given in the Supporting Information. (+)-(*S*)- $\alpha$ -methoxy- $\alpha$ -(trifluoromethyl)-phenylacetyl chloride was obtained from Alfa-Aesar (>98%,

(+)-137.3°).  $^1\text{H}$ ,  $^{13}\text{C}\{^1\text{H}\}$ , and  $^{19}\text{F}$  NMR spectra and  $^1\text{H}$ - $^{15}\text{N}$  HMBC experiments were collected either on a Bruker DRX-400 spectrometer, Bruker Avance III 600 spectrometer, or an Agilent MR 400 spectrometer.  $^{15}\text{N}$  NMR chemical shifts are referenced to a nitromethane external standard.  $[\alpha]_{\text{D}}$  values were measured on a ATAGO AP-300 polarimeter at 23 °C.

**$^{19}\text{F}$  NMR Spectroscopic Determination of Enantiomeric Excess.** The cyclic amine, (+)-(*S*)- $\alpha$ -methoxy- $\alpha$ -(trifluoromethyl)-phenylacetyl chloride (1.2 equiv), and  $\text{NEt}_3$  (5.0 equiv) were allowed to react in benzene. Evaporation of volatile materials after 1 h, followed by pentane extraction (3  $\times$  4 mL) gives a colorless oil. Integration of  $^{19}\text{F}$  NMR (60 °C,  $\text{CDCl}_3$ ) signals for racemic- and optically-enriched samples provided data to determine % ee.

**HPLC Analysis of Enantioselectivity.** The % ee was determined by HPLC analysis (flow rate = 1.0 mL/min,  $\lambda$  = 254 nm) using Regis (*S,S*)-Whelk O1 column (column dimensions = 25 cm  $\times$  4.6 mm i.d., Spherical Kromasil Silica, particle size = 5  $\mu\text{m}$ , 100 Å). The chiral pyrrolidines and piperidines were converted to benzoyl derivative prior to HPLC analysis. Pure samples of cyclic imines were used to determine their enantiomeric excesses by HPLC.

**4-Allyl-2-methyl-4-(4-bromophenyl)pyrrolidine (4b).**  $\{S-1\}$ -Zr( $\text{NMe}_2$ )<sub>2</sub> (0.120 g, 0.196 mmol), benzene (30 mL), and **4a** (0.549 g, 1.96 mmol) were stirred at room temperature for 4 h. Vacuum distillation of the reaction mixture provided the product **4b** (bp 120–125 °C, 0.1 mmHg) in excellent yield (0.398 g, 1.42 mmol, 94.3%). The isolated **4b** was a mixture of *cis* and *trans* diastereomers (*cis:trans* = 4:1; ee (*cis*) = 97%, ee (*trans*) = 95%) determined by  $^{19}\text{F}$  NMR spectroscopy.  $^1\text{H}$  NMR (chloroform-*d*<sub>1</sub>, 400 MHz):  $\delta$  7.43–7.40 (m,  $\text{C}_6\text{H}_4\text{Br}$ ), 7.10–7.02 (m,  $\text{C}_6\text{H}_4\text{Br}$ ), 5.49–5.39 (m,  $\text{CH}=\text{CH}_2$ ), 4.97–4.91 (m,  $\text{CH}=\text{CH}_2$ ), 3.51–3.42 (m,  $\text{CHMeNH}$ ), 3.20–3.17 (m,  $\text{CH}_2\text{NH}$ ), 2.58 (br, NH), 2.43–2.33 (m,  $\text{CH}_2\text{CH}=\text{CH}_2$ ), 2.28–2.24 (m,  $\text{CH}_2\text{CHMe}$ ), 1.59–1.53 (m,  $\text{CH}_2\text{CHMe}$ ), 1.22 (d,  $^3J_{\text{HH}} = 6.0$  Hz,  $\text{CHMeNH}$ ), 1.17 (d,  $^3J_{\text{HH}} = 6.0$  Hz,  $\text{CHMeNH}$ ).  $^{13}\text{C}\{^1\text{H}\}$  NMR (100 MHz, chloroform-*d*<sub>1</sub>):  $\delta$  146.48 ( $\text{C}_6\text{H}_4\text{Br}$ ), 146.20 ( $\text{C}_6\text{H}_4\text{Br}$ ), 134.80 ( $\text{CH}=\text{CH}_2$ ), 134.60 ( $\text{CH}=\text{CH}_2$ ), 131.38 ( $\text{C}_6\text{H}_4\text{Br}$ ), 131.29 ( $\text{C}_6\text{H}_4\text{Br}$ ), 128.89 ( $\text{C}_6\text{H}_4\text{Br}$ ), 128.88 ( $\text{C}_6\text{H}_4\text{Br}$ ), 119.93 ( $\text{C}_6\text{H}_4\text{Br}$ ), 119.90 ( $\text{C}_6\text{H}_4\text{Br}$ ), 118.03 ( $\text{CH}=\text{CH}_2$ ), 117.94 ( $\text{CH}=\text{CH}_2$ ), 57.94 ( $\text{CH}_2\text{NH}$ ), 57.15 ( $\text{CH}_2\text{NH}$ ), 54.26 ( $\text{CHMeNH}$ ), 53.33 ( $\text{CHMeNH}$ ), 51.90 ( $\text{C}(\text{C}_6\text{H}_4\text{Br})$ ), 51.84 ( $\text{C}(\text{C}_6\text{H}_4\text{Br})$ ), 47.24 ( $\text{CH}_2\text{CH}=\text{CH}_2$ ), 46.0 ( $\text{CH}_2\text{CH}=\text{CH}_2$ ), 45.63 ( $\text{CH}_2\text{CHMe}$ ), 45.38 ( $\text{CH}_2\text{CHMe}$ ), 22.40 ( $\text{CHMe}$ ), 22.21 ( $\text{CHMe}$ ).  $^{15}\text{N}$  NMR (chloroform-*d*<sub>1</sub>, 61 MHz):  $\delta$  -346.2, -347.5 MS (ESI) exact mass calcd for  $\text{C}_{14}\text{H}_{18}\text{BrN}$ :  $m/z$  280.0695 ( $[\text{M}^+ + \text{H}^+]$ ); found: 280.0700. ( $\Delta$  -1.65 ppm).  $[\alpha]_{\text{D}}^{23} = -34.3^\circ$  ( $\text{C}_6\text{H}_6$ ).

**3-(But-2-ynyl)-5-ethyl-3,4-dihydro-3-phenyl-2H-pyrrole (9b).**  $\{S-1\}$ -Zr( $\text{NMe}_2$ )<sub>2</sub> (0.100 g, 0.163 mmol) and **9a** (0.367 g, 1.63 mmol) were stirred in benzene (25 mL) at room temperature for 4 h. All the volatiles were removed by rotary evaporation to provide a light yellow oil, which was purified by flash chromatography (silica gel, hexane:EtOAc = 2:1) to yield **9b** as a colorless oil (0.349 g, 1.55 mmol, 95.1% yield, 87% ee).  $^1\text{H}$  NMR (chloroform-*d*<sub>1</sub>, 400 MHz):  $\delta$  7.35–7.30 (m, 2 H,  $\text{C}_6\text{H}_5$ ), 7.27–7.19 (m, 3 H,  $\text{C}_6\text{H}_5$ ), 4.19 (m, 1 H,  $\text{CH}_2\text{N}$ ), 4.00 (m, 1 H,  $\text{CH}_2\text{N}$ ), 2.97 (m, 1 H,  $\text{CH}_2\text{C}(\text{Et})\text{N}$ ), 2.85 (m, 1 H,  $\text{CH}_2\text{C}(\text{Et})\text{N}$ ), 2.41 (q,  $^5J_{\text{HH}} = 2.5$  Hz, 2 H,  $\text{CH}_2\text{CC}$ ), 2.39 (q,  $^3J_{\text{HH}} = 7.6$  Hz, 2 H,  $\text{CH}_2\text{CH}_3$ ), 1.73 (t,  $^5J_{\text{HH}} = 2.5$  Hz, 3 H,  $\text{CH}_3$ ), 1.19 (t,  $^3J_{\text{HH}} = 7.6$  Hz, 3 H,  $\text{CH}_2\text{CH}_3$ ).  $^{13}\text{C}\{^1\text{H}\}$  NMR (chloroform-*d*<sub>1</sub>, 100 MHz):  $\delta$  179.1 ( $\text{CH}_2\text{C}(\text{Et})\text{N}$ ), 147.2 ( $\text{C}_6\text{H}_5$ ), 128.4 ( $\text{C}_6\text{H}_5$ ), 126.9 ( $\text{C}_6\text{H}_5$ ), 126.2 ( $\text{C}_6\text{H}_5$ ), 77.8 ( $\text{CCH}_3$ ), 76.4 ( $\text{CH}_2\text{C}$ ), 71.6 ( $\text{CH}_2\text{N}$ ), 50.0 ( $\text{C}(\text{Ph})\text{CH}_2\text{CCCH}_3$ ), 48.9 ( $\text{CH}_2\text{C}(\text{Et})\text{N}$ ), 32.5 ( $\text{CH}_2\text{CC}$ ), 27.1 ( $\text{CH}_2\text{CH}_3$ ), 10.5 ( $\text{CH}_2\text{CH}_3$ ), 3.7 ( $\text{CH}_3$ ).  $^{15}\text{N}$  NMR (chloroform-*d*<sub>1</sub>, 61 MHz):  $\delta$  -219.8. MS (ESI) exact mass calcd for  $\text{C}_{16}\text{H}_{20}\text{N}$ :  $m/z$  226.1596 ( $[\text{M}^+ + \text{H}^+]$ ); found: 226.1594.  $[\alpha]_{\text{D}}^{23} = +30.4^\circ$  ( $\text{C}_6\text{H}_6$ ).

## ■ ASSOCIATED CONTENT

### Supporting Information

Synthetic, catalytic, and kinetics procedures, tables with HPLC conditions, and data for evaluating optical purity, configuration assignments. This material is available free of charge via the Internet at <http://pubs.acs.org>.

## ■ AUTHOR INFORMATION

### Corresponding Author

sadow@iastate.edu

### Present Address

<sup>†</sup>Department of Chemistry, University of Chicago, 5735 S. Ellis Ave., Chicago, IL 60637.

### Notes

The authors declare no competing financial interest.

## ■ ACKNOWLEDGMENTS

This research was supported by the U.S. Department of Energy, Office of Basic Energy Sciences, Division of Chemical Sciences, Geosciences, and Biosciences through the Ames Laboratory (contract no. DE-AC02-07CH11358). Prof. M. Jeffries-EL is thanked for generous access to an HPLC.

## ■ REFERENCES

- (1) Hong, S.; Marks, T. J. *Acc. Chem. Res.* **2004**, *37*, 673.
- (2) Müller, T. E.; Hultzs, K. C.; Yus, M.; Foubelo, F.; Tada, M. *Chem. Rev.* **2008**, *108*, 3795.
- (3) Togni, A.; Grützmaier, H. *Catalytic heterofunctionalization: from hydroamination to hydrozirconation*; 1st ed.; Wiley-VCH: Weinheim, 2001.
- (4) Hannedouche, J.; Schulz, E. *Chem.—Eur. J.* **2013**, *19*, 4972.
- (5) Li, Y.; Marks, T. J. *J. Am. Chem. Soc.* **1998**, *120*, 1757.
- (6) Molander, G. A.; Dowdy, E. D.; Pack, S. K. *J. Org. Chem.* **2001**, *66*, 4344.
- (7) Gribkov, D. V.; Hultzs, K. C.; Hampel, F. *J. Am. Chem. Soc.* **2006**, *128*, 3748.
- (8) Zhai, H.; Borzenko, A.; Lau, Y. Y.; Ahn, S. H.; Schafer, L. L. *Angew. Chem., Int. Ed.* **2012**, *51*, 12219.
- (9) Fujii, K. *Chem. Rev.* **1993**, *93*, 2037.
- (10) Trost, B. M.; Jiang, C. *Synthesis* **2006**, 369.
- (11) La, D. S.; Alexander, J. B.; Cefalo, D. R.; Graf, D. D.; Hoveyda, A. H.; Schrock, R. R. *J. Am. Chem. Soc.* **1998**, *120*, 9720.
- (12) Lee, J. Y.; You, Y. S.; Kang, S. H. *J. Am. Chem. Soc.* **2011**, *133*, 1772.
- (13) Aikawa, K.; Okamoto, T.; Mikami, K. *J. Am. Chem. Soc.* **2012**, *134*, 10329.
- (14) Yao, L.; Liu, K.; Tao, H.-Y.; Qiu, G.-F.; Zhou, X.; Wang, C.-J. *Chem. Commun.* **2013**, 49, 6078.
- (15) Zhou, F.; Guo, J.; Liu, J.; Ding, K.; Yu, S.; Cai, Q. *J. Am. Chem. Soc.* **2012**, *134*, 14326.
- (16) Willis, M. C.; Powell, L. H. W.; Claverie, C. K.; Watson, S. J. *Angew. Chem., Int. Ed.* **2004**, *43*, 1249.
- (17) Trost, B. M.; Machacek, M. R.; Aponick, A. *Acc. Chem. Res.* **2006**, *39*, 747.
- (18) Zhao, Y.; Rodrigo, J.; Hoveyda, A. H.; Snapper, M. L. *Nature* **2006**, *443*, 67.
- (19) Ward, R. S. *Chem. Soc. Rev.* **1990**, *19*, 1.
- (20) Manna, K.; Everett, W. C.; Schoendorff, G.; Ellern, A.; Windus, T. L.; Sadow, A. D. *J. Am. Chem. Soc.* **2013**, *135*, 7235.
- (21) Manna, K.; Kruse, M. L.; Sadow, A. D. *ACS Catal.* **2011**, *1*, 1637.
- (22) Manna, K.; Xu, S.; Sadow, A. D. *Angew. Chem., Int. Ed.* **2011**, *50*, 1865.
- (23) Martinez, P. H.; Hultzs, K. C.; Hampel, F. *Chem. Commun.* **2006**, 2221.
- (24) Wood, M. C.; Leitch, D. C.; Yeung, C. S.; Kozak, J. A.; Schafer, L. L. *Angew. Chem., Int. Ed.* **2007**, *46*, 354.
- (25) Jiang, T.; Livinghouse, T. *Org. Lett.* **2010**, *12*, 4271.
- (26) Jiang, T.; Livinghouse, T.; Lovick, H. M. *Chem. Commun.* **2011**, 47, 12861.
- (27) Kim, J. Y.; Livinghouse, T. *Org. Lett.* **2005**, *7*, 4391.
- (28) Mourad, A. K.; Leutzow, J.; Czekelius, C. *Angew. Chem., Int. Ed.* **2012**, *51*, 11149.

- (29) Iska, V. B. R.; Verdolino, V.; Wiest, O.; Helquist, P. *J. Org. Chem.* **2010**, *75*, 1325.
- (30) Hong, S.; Tian, S.; Metz, M. V.; Marks, T. J. *J. Am. Chem. Soc.* **2003**, *125*, 14768.
- (31) Glueck, D. S. *Catal. Sci. Technol.* **2011**, *1*, 1099.
- (32) Gagne, M. R.; Stern, C. L.; Marks, T. J. *J. Am. Chem. Soc.* **1992**, *114*, 275.
- (33) Christoffers, J.; Baro, A. *Adv. Synth. Catal.* **2005**, *347*, 1473.
- (34) Lebsack, A. D.; Link, J. T.; Overman, L. E.; Stearns, B. A. *J. Am. Chem. Soc.* **2002**, *124*, 9008.
- (35) Wolfsberg, M. *Acc. Chem. Res.* **1972**, *5*, 225.
- (36) Parkin, G. *Acc. Chem. Res.* **2009**, *42*, 315.
- (37) Sperger, C. A.; Fiksdahl, A. *J. Org. Chem.* **2010**, *75*, 4542.